doi:10.1016/j.gca.2004.06.001

Kinetic control of oxidation state at thermodynamically buffered potentials in subsurface waters

JOHN W. WASHINGTON,[1,]* DINKU M. ENDALE,[2] LIDIA P. SAMARKINA,[1] and KARI E. CHAPPELL[1]

[1]U.S. Environmental Protection Agency, National Exposure Research Laboratory, 960 College Station Road, Athens, Georgia 30606, USA
[2]United States Department of Agriculture-Agricultural Research Service, J. Phil Campbell, Sr., Natural Resource Conservation Center, 1420 Experiment Station Road, Watkinsville, Georgia 30677, USA

Abstract—Dissolved oxygen (DO) and organic carbon (C_{org}) are among the highest- and lowest-potential reactants, respectively, of redox couples in natural waters. When DO and C_{org} are present in subsurface settings, other couples are drawn toward potentials imposed by them, generating a bimodal clustering of calculated redox potentials. Which cluster a couple is drawn toward is determined by whether the couple's oxidant or reductant is more concentrated. Generally, reactants $>10^{-6}$M are near equilibrium with their dominant complementary reactant and in a cluster, whereas reactants $<10^{-6}$M are relatively slow to react and diverge from the clusters. These observations suggest that reactions of higher-potential oxidants with lower-potential reductants commonly proceed simultaneously, regardless of the presence of other potential reactants, with the rates of reaction being determined more by concentration than relative potentials. As DO or C_{org} decreases, the potential gap separating couples diminishes. In waters having quantifiable concentrations of higher potential oxidants O_2 and NO_3^-, [H_2] was not diagnostic of their presence. In the water we analyzed having no quantifiable O_2 or NO_3^-, redox potential calculated with [H_2] was similar to potentials calculated for SO_4^{2-} reduction and methanogenesis. Composite reactions, $NO_3^- \rightarrow N_2$ and $O_2 \rightarrow H_2O$, are best characterized in multiple steps due to slow reaction of low-concentration intermediates. The [CO] data we report, among the first for groundwater, are high compared to water equilibrated with the atmosphere. *Copyright © 2004 Elsevier Ltd*

1. INTRODUCTION

Among the state variables required to define the chemistry of environmental systems, electron potential has been uniquely elusive to characterize and challenging to model. Some early studies of redox reported promising clarity of results. For example, working with marine sediments, Berner (1963) described consistency between measured values of redox and those calculated based on S speciation. Thorstenson (1970) sampled several reducing environments and found consistence in calculated redox for S and N couples. In concentrated acidic mine drainage, Nordstrom et al. (1979) reported redox consistence between measured redox and potentials calculated for Fe complexes.

The record of success for agreement among independent methods for evaluating electron potential is best regarded as spotty, however, because there are many examples reporting inconsistent results as well. The complexity of relationships among redox couples was brought home most clearly in the seminal paper of Lindberg and Runnells (1984), who reported measured and calculated redox values for several couples gleaned from a USGS national database of groundwater chemistry. They observed that measured redox did not correspond with calculated values, nor did calculated redox values all agree among each other (Lindberg and Runnells, 1984). These researchers concluded that neither measured E_H, nor any single calculated E_H, represents "a master redox value for the water."

Such limitations using thermodynamics led researchers to

propose classifying redox settings based on the terminal electron-accepting process (TEAP) (Lovley and Goodwin, 1988). According to TEAP, microbes first ferment complex organic molecules to simpler intermediate compounds such as acetate, formate and H_2. In turn, these intermediates are oxidized by respiration with terminal electron acceptors (TEAs). According to this model, redox can be characterized by inferring the TEAP from measured [H_2] because each TEA supports a characteristic [H_2] (Lovley and Goodwin, 1988). In general, NO_3^- reduction is thought able to proceed at [H_2] $<$ 0.1 nM, Fe(III) reduction at [H_2] $\sim$ 0.2 to 0.8 nM, SO_4^{2-} reduction at [H_2] $\sim$ 1 to 4 nM, and CO_2 reduction at 5 to 30 nM (Chapelle et al., 1997). Early investigators argued that [H_2] varies with TEAP because microbes that enjoy the energetic advantage of reactions having higher standard-state free energies competitively exclude (CETEAP) other microbes by suppressing H_2 to concentrations too low to sustain their rivals (Lovley and Phillips, 1987). Still others argue that [H_2] varies with TEAP by a partial equilibrium process (PETEAP) wherein slow fermentation is followed by fast respiration for all TEAs. For PETEAP, the high concentrations of higher-energy TEAs, such as Fe(III), can poise the system at high oxidation states where only low [H_2] is stable and lower-energy TEAs, such as SO_4^{2-}, are not thermodynamically inclined to substantial reduction (Postma and Jakobsen, 1996).

The TEAP paradigm does not address directly the oxidation of reductants other than fermentation products, nor does it address reduction of TEAs by anything but fermentation products. Yet there are many other significant redox processes taking place in natural systems: inorganic solutes can react abiotically, e.g., Fe^{2+} with dissolved O_2 (Singer and Stumm,

---

* Author to whom correspondence should be addressed (washington.john@epa.gov).

1970); organic solutes can react abiotically, e.g., degradation of organic C (C_{org}) to CO (Conrad and Seiler, 1985); inorganic solutes can react with surfaces abiotically, e.g., H_2S with Fe(III) oxides (Rickard, 1974); organic solutes can react with surfaces abiotically, e.g., humic material with Fe(III) oxides (Lovley et al., 1996); and there are numerous biologically mediated reactions carried out by autotrophs in the subsurface (Stevens, 1997). Recognition that these general kinds of reactions can take place has led to modeling efforts based on local partial equilibrium (LPE) in which species subsets, often high-concentration solutes, are modeled as in equilibrium with each other (e.g., Morel and Hering, 1993; Lichtner, 1996). However, success of LPE models has been limited because understanding of specific interactions among couples remains elusive (e.g., McNab and Narasimhan, 1994).

To help elucidate those factors and processes controlling the nature and extent of reaction between redox couples in subsurface waters, we sampled waters from four dissimilar settings, and monitored one location for 2 yr. We subjected these waters to analysis for a wide array of redox-sensitive analytes and analyzed the resulting data thermodynamically.

2. MATERIALS AND METHODS

2.1. Site Descriptions

Waters were sampled from four subsurface-flow-system sources located in the Southern Piedmont Physiographic Province, Oconee County, in northeastern Georgia, and at all sample locations, bedrock is gneiss (Railsback et al., 1996), and the lithologic unit is designated as Athens Gneiss. Based on well cuttings and outcrops in the study area, Athens Gneiss predominantly is granodioritic gneiss locally. Soil series are comprised mostly of Cecil series and Pacolet series, both classified clayey, kaolinitic, thermic Typic Kanhapludult.

Three of the sample locations are on USDA Agricultural Research Service property, the J. Phil Campbell, Sr., Natural Resource Conservation Center (Amirtharajah et al., 2002), ~10 km south of the EPA lab in Athens, Georgia, where the analyses were performed. Well NU18 and Spring SpW2 are ~60 m apart. They combine to represent midflow path and discharge locations, respectively, of the USDA Watershed 2, an area of ~10 ha. This watershed, encompassed entirely within USDA property, is comprised of pasture through which ~100 cow-calf pairs are rotated roughly one week in six. In addition to nutrients and C_{org} from cattle waste, Watershed 2 also is fertilized at a rate of ~78 kg N/(ha-yr). The uppermost aquifer flow is through the saprolite, which ranges from about <8 m to >21 m depth. Spring SpW2 was sampled for most analytes one to more than 2 dozen times over about 2 yr. Well NU18 extends to the top of bedrock, 11 m, and is screened over the bottom 3 m. Application of the Jacob straight-line drawdown method (Driscoll, 1989) to pumping test data from Well NU18 led to a hydraulic conductivity of ~2 x 10^{-5} to 3 x 10^{-5} cm/s. The hydraulic gradient between NU18 and SpW2 ranges from ~0.02 to 0.04.

Spring NWSp is about 1 km NNW of Spring SpW2 in a wooded area of the USDA property. It is similar to Spring SpW2 except that it issues from an area used less intensively for agriculture and in which no cattle are grazed.

The Hillcrest Well, a public water-supply well drilled into granodioritic gneiss to a depth of ~177 m, is located ~3.5 km west of USDA Watershed 2. It was sampled from a tap on the well head during its normal, continuous-production pumping of ~340 L/min.

2.2. Analytical Methods

For springs, an effort was made to transfer the water from as near to the source of issuance as possible by syphoning or peristaltic pumping into a container where flow was from the bottom upwards, spilling over the container lip continuously so that samples could be collected having virtually no contact with the air. For wells, samples were collected only after stable readings were achieved for pH (Orion Model 250A+),

specific conductance (YSI Model 30), dissolved O_2 (YSI Model 55), and temperature (using thermocouples on the pH, specific conductance and O_2 probes); these samples also were collected from an upwelling, overflowing container. YSI reports the detection limit for the Model 55 dissolved O_2 probe to be 9 μM, a conservatively high value that varies between meters and with wear on the sensor membrane.

In addition to the field-monitoring parameters listed above, alkalinity was measured on-site by titration with a LaMotte alkalinity kit and/or Chemetrics' Titret reverse titration kits. Nitrite was measured on-site using a Hach 2010 spectrometer by a diazotization method for which nitrite is reacted with Hach-prepared sulfanilic acid to form a diazonium salt and then with chromotropic acid to form a colored complex that absorbs light at $\lambda = 507$ nm. We discovered that exposure of these colorimetric solutions to sunlight induces a photolytic reaction that registers an artifactually high absorbance; this effect was not observed upon exposure to any of a variety of artificial lights tested. Consequently, great care was exercised to avoid sample exposure to sunlight in the field. The internal spectrometer calibration was checked against standards and found to agree quantitatively down to 0.3 μM and to have an estimated detection limit (i.e., detect concentrations as a difference from zero) of 0.2 μM. Multiple measurements routinely were made on each of duplicate samples for which the matched blank, and sample spectrometric cells were switched between samples, or multiple matched pairs of cells were used. In all cases, closely consistent readings were observed. Sulfide was measured on-site using the Hach 2010 spectrometer by the methylene blue method (Clesceri et al., 1998) with Hach-prepared N, N-dimethyl-p-phenylenediamine oxalate, and absorbance was read at $\lambda = 665$ nm. The internal spectrometer calibration was checked against standards and found to have an estimated detection limit (i.e., detect concentrations as a difference from zero) of 0.03 μM. Multiple measurements routinely were made on each of duplicate samples for which the blank and sample spectrometric cells were switched between samples, or multiple matched pairs of cells were used. In all cases, closely consistent readings were observed.

2.2.1. Iron sampling and analyses

Three or more replicate samples were collected to represent each Fe analysis. For each replicate, 8 to 10 μL of concentrated HCl was pipetted into acid-washed, 50-mL, crimp-seal, glass serum bottles, the bottles were capped with Teflon caps and crimp sealed, then flushed with Grade 5 N_2 (99.999% purity) for 1 min. This flushing time assured that O_2 was purged from the jars and that sufficient HCl remained unevaporated so that 5-mL samples would be preserved at $1.7 < pH < 2$. On-site, ~6 mL of water was drawn from the upwelling sample container through a needle into a gas-tight, Teflon-plunger syringe graduated to 5 mL. The needle was removed, a 0.2 μm syringe filter was emplaced and the needle replaced. Gas bubbles, if any, were tapped to the top and the first ~1 mL was discarded to purge the bubbles and saturate the filter, the next 5 mL were injected into the serum bottles and the sample swirled. With this care, water samples were not exposed to air before complete acidification to pH < 2 nor until uncrimping the serum jars immediately before analysis.

In the lab, Fe analyses were conducted by the ferrozine procedure (Stookey, 1970) that included Fe(III) reduction with hydroxylamine hydrochloride after the method of Viollier et al. (2000) with a modification to the interpretation of the analytical results: the A_1 reading, representing the absorbance of the sample reacted with the ferrozine, was taken as representing $[Fe^{2+}]$; and the A_2 reading, representing the absorbance of the A_1 solution after reacting with hydroxylamine hydrochloride and ammonium hydroxide buffer, was interpreted as representing total [Fe]. Subtraction of the $[Fe^{2+}]$ value from the dilution-corrected total [Fe] described [Fe(III)]. These variations from Viollier et al. (2000) are necessary because it was discovered that the A_1 readings, which were interpreted in the original reference as $\lambda = 562$ nm light absorbance in the standards, instead was light scattering by freshly precipitated ferric colloids. This light scattering was confirmed by preparing ferric standards as described in Viollier et al. (2000) by dilution of commercial stock of [Fe(III)] = 1000 ppm in water to the 1-ppm range, which increased pH by about 3 units; immediately measured absorbances were similar to Viollier et al. (2000), but, after settling overnight, resulting absorbances were near zero and a yellowish-brown precipitate of colloidal Fe(III) had settled on the bottoms of

the cuvettes. All samples in this study had $[Fe^{2+}]$ well in excess of detection limits; the estimated ferric detection limit was 0.4 μM. In this study, three to five acid-stabilized $[Fe(III)]$ standards were analyzed with each sampling run.

2.2.2. Anion sampling and analyses

Three replicate samples were collected for major-anion analysis. Anion samples were stored in the spring pool in the field, then preserved in the lab by freezing until analysis. Analysis for Cl^-, NO_2^-, NO_3^-, SO_4^{2-}, and $H_2PO_4^-$ routinely was performed using a Dionex DX-500 ion chromatograph with an ASRS Ultra electrolytical suppressor, Dionex Ionpac standard-bore AS-15 guard and separating columns, and an anion trapping column to suppress carbonate. An eluent mix, flowing at 1.5 mL/min, was ramped from 2% 0.1 M NaOH in degassed deionized H_2O to 60%. Standard curves consisted of five to seven standards depending on the analyte. Check standards and blanks were included in every run, and all injections were 100 μL. The analytes Cl^-, NO_3^-, and $SO_4^=$ were detected in all study samples. The detection limits for NO_2^- and $H_2PO_4^-$ were too high to detect these solutes by this method for most samples. It is this limitation that necessitated the above-described spectrometric method for NO_2^-.

In an attempt to detect $H_2PO_4^-$, selected samples were run using a Dionex DX-500 ion chromatograph with an AMMS III chemical suppressor, and Dionex Ionpac microbore, AS-16 guard and separating columns. An eluent mix, flowing at 1.0 mL/min, was ramped from 30% 0.05 M NaOH in degassed deionized H_2O to 60% over 30 min. All injections were 1000 μL. Standards were run at 1 and 0.10 μM $H_2PO_4^-$ with strong peaks expressed at both concentrations. The selected samples exhibited no quantifiable peaks for $H_2PO_4^-$.

2.2.3. Ammonium sampling and analyses

Ammonia was present in the mildly acidic samples of this study dominantly as NH_4^+. The three replicate samples that were collected and preserved by freezing for anions also were used for NH_4^+ analysis. Ammonia was analyzed by Accumet ammonia ion selective electrode or the phenate method (Clesceri et al., 1998) wherein ammonia is reacted with hypochlorite and phenol to form indophenol blue, the intensity of which is read spectrometrically at $\lambda = 640$ nm. Common standards were measured using both methods to assure consistent results. Detection limits with the electrode were highly variable (Appendix Table 1B); the detection limit for the phenate method was 0.6 μM. Fresh calibration standards and blanks were prepared and analyzed repetitively each time NH_4^+ was analyzed.

2.2.4. Dissolved N_2O, H_2 and CO_2 sampling and analysis

Two gas-sampling jars were constructed of thick-walled glass, total volume was ~1200 mL with graduations to 1000 mL. In each jar, a glass stopcock was placed at about the 1000-mL mark above a Teflon septum at ~800 mL, which was over a second glass stopcock at 300 mL. The jars were capped with thick-walled, Teflon, screw-on caps. Before sampling these jars were flushed with Grade 5 or Grade 5.5 (99.9995%) N_2. To assure dissolved-gas-sample integrity, the last task performed in the field was gas-sample collection. To collect samples for dissolved gases, the lower stopcock was connected to a flowing Tygon tube and both stopcocks were opened allowing the jars to fill to ~900 mL. With samples collected, to minimize potential gas loss, the gas-sampling jars were stowed on their sides so that both stopcocks, the Teflon septum, and the cap all were submerged, and the gas headspace was exposed solely to the thick-walled glass.

At the lab, the water sample and headspace were equilibrated by vigorous shaking for 1 min. A single 5-mL headspace sample was used to analyze N_2O, H_2, and CO_2 simultaneously. Headspace samples were injected into an AT 6890 gas chromatograph (GC) with two 2-mL sampling loops in series attached by two ten-port valves that separated flow to: (1) a Hayesep Q column (4 ft x 1/8 in o.d., 80/100 mesh) attached to a 5-ft Hayesep N column (6 ft x 1/8 in o.d., 80/100 mesh), then to a micro electron-capture detector (μECD) using a 95% Ar/5% CH_4 carrier gas; and (2) a Hayesep DB-packed column (30 ft x 1/8 in o.d., 80/100 mesh) leading to a thermal-conductivity detector (TCD) using Grade 5 He (99.999% purity). Headspace $[N_2O]$ was measured using the μECD, similar to the method of Mosier and Mack (1980).

Headspace $[H_2]$ and $[CO_2]$ were measured using the TCD. Standard curves, usually four- or five-point, were constructed periodically using Scotty standard mixes; multiple check standards were injected during every sampling round. Headspace $[H_2]$ commonly was checked with a Trace Analytical model RGA3 GC equipped with a reduction gas analyzer (RDA) as described in Mazur and Jones (2001). Values of $[H_2]$ agreed well between the two methods. Original dissolved-gas concentrations were calculated from headspace concentrations using Henry's Law functions reported in Wilhelm et al. (1977). With this approach: (1) headspace N_2O could be measured to below atmospheric background of ~310 ppb by volume (ppbv); (2) headspace H_2 could be measured to ~40 ppbv and was limited largely by H_2 impurities in the N_2 gas used to fill the jar headspace; and 3) headspace CO_2 could be measured to well below the range of values measured in any sample.

2.2.5. Dissolved CO sampling and analysis

Headspace $[CO]$ was measured using samples drawn from the gas-sampling jars described above in 2.2.4. These headspace samples were analyzed on the Trace Analytical model RGA3 GC equipped with an RDA as described in Mazur and Jones (2001). Sample and standard injection volume was 3 mL. A National Institute of Standards and Technology (NIST)-traceable standard periodically was mixed in selected fractions with Grade 5 N_2 to confirm linear detector response and the NIST standard was injected several times in each sampling round. Original dissolved $[CO]$ was calculated from headspace $[CO]$ using Henry's Law functions (Wilhelm et al., 1977). With this approach CO in the headspace could be measured to well below the range of values measured in any sample.

2.2.6. Dissolved CH_4 sampling and analysis

Headspace $[CH_4]$ was measured using samples drawn from the gas-sampling jars described above in 2.2.4. These headspace samples were analyzed on an HP 5890 GC equipped with a flame ionization detector as described in Mazur and Jones (2001). Sample and standard injection volume was 0.3 or 0.5 mL. Outdoor air was injected as a standard several times with each sampling round and taken as $[CH_4] = 1.839$ ppmv (http://cdiac.esd.ornl.gov/). Scotty standard gases were mixed in selected fractions with Grade 5 N_2 to confirm linear detector response. Original dissolved $[CH_4]$ was calculated from headspace $[CH_4]$ using Henry's Law functions (Wilhelm et al., 1977). With this approach, headspace $[CH_4]$ could be measured to ~0.02 ppmv, but the detection limit varied between sampling runs.

2.2.7. Organic carbon sampling and analysis

C_{org} was analyzed on single samples composited from the three replicate samples that were collected for major-anion analysis. The samples had been preserved in the lab by freezing until analysis. Before analysis, standards and samples were dosed to 1% HCl by volume to facilitate purging of inorganic carbon. Samples were analyzed three to five times each on a Shimadzu 5050A Total Organic Carbon Analyzer. Standard curves consisted of three to five standards. In all samples, $[C_{org}]$ was well in excess of the lowest standard. Check standards and blanks were included in every run.

2.3. Determining [Fe(III)]-Controlling Solid Phases

In February 2001, saprolitic borehole cuttings were collected during auger drilling of a new monitoring well on USDA Watershed W2, roughly 80 m south of Well NU18. The cuttings represent an interval of ~7 to 11 m below ground level and ~1 m and more below static water level in the monitoring well. These cuttings were collected on the day of drilling by digging through the cuttings pile to less-exposed material and transferring them to a 20-L plastic bucket with a tightly sealing lid. Because of their saturated state, the cuttings were immersed below ~5 cm of aquifer water when the transfer was complete. The cuttings were transported to the lab immediately, the balance of the bucket filled with degassed deionized water, the bucket sealed and placed in a dark walk-in cooler for storage at ~5 C.

In April 2002, ~500 g of cuttings were collected from the bottom middle of this bucket and transferred to about a liter of pH = 1.7 HCl,

and this suspension was kept on a magnetic stirrer. The solids to liquid ratio and pH was chosen to assure that solid phases would not be depleted by dissolution so that equilibrium constants might be inferred. Maintenance at pH < 2 by addition of concentrated HCl kept oxidation of Fe^{2+} at a low rate (Singer and Stumm, 1970) so that mineral-Fe speciation could be deduced from the liberated Fe that was measured by the above-described method (2.2.1).

2.4. Calculating Activity Coefficients

Activity coefficients were calculated for these analytes using the Extended Debye-Huckel Equation (Stumm and Morgan, 1996), which requires calculation of the ionic strength ($I = 0.5 \Sigma m_i z_i^2$ where m is molarity and z is ion charge). The major anionic species were analyzed on IC but the dominant cationic species in these samples have not been analyzed. Major cation distribution was estimated from analyses for 14 samples of Spring SpW2 waters (Thomas Meixner, University of California, Riverside, personal communication) collected during Spring 2001. For these 14 analyses, the relative concentrations of the major cations varied little. Reporting millimolarity according to mean $\pm$ 1 standard deviation: $[Ca^{2+}] = 0.09 \pm 0.02$; $[Mg^{2+}] = 0.12 \pm 0.04$; $[Na^+] = 0.13 \pm 0.03$; $[K^+] = 0.16 \pm 0.01$. Ionic strength was calculated by assuming the above cationic ratios for the samples in this study and charge equating these cationic compositions to the measured anionic concentrations.

3. ANALYTICAL RESULTS

Analytical results are tabulated as Appendix Tables 1A and 1B. Comparing sample locations drawing from cattle-grazing areas (Well NU-18, Spring SpW2) to those in which no cattle are grazed (Hillcrest Well, Spring NWSp), $[NO_3^-]$ was higher in grazed-source samples. The conductance was higher in grazed-source samples than the nongrazed, saprolitic-source sample (Spring NWSp), suggesting higher dissolved solids in samples from grazed areas. Also, the pH of samples from the outlet of the grazed watershed, Spring SpW2, was lower than other sample sources; we conjecture that this is caused by high $H_2CO_3^*$, a consequence of relatively high fugacity of CO_2 (f_{CO2}), in turn caused by high microbial activity due to the high flux of organic substrate from manure.

The Hillcrest well had much higher specific conductance, pH, alkalinity, and $[Fe^{2+}]$, and lower $[O_2]$, $[N_2O]$, and $[NO_3^-]$ than saprolitic sample sources. This well is the only sample location drawing water from the deeper, consolidated-rock aquifer. The lower values for the generally surficial-source $[O_2]$, $[N_2O]$, and $[NO_3^-]$ likely reflect the deeper flow pattern of the rock aquifer.

There are few literature data, if any, for [CO] in groundwater other than the values we report here (Appendix Table 1A). Atmospheric background for CO is ~100 ppbv (cdiac@ornl.gov). Assuming rainfall equilibrates with this concentration, a unitless Henry's Law value of $K_H^{CO} \sim 0.027$ (Wilhelm et al., 1977) gives a typical rainfall value of [CO] ~ 0.12 nM. CO concentrations we measured ranged from 7 to 200 times this atmosphere-equilibrated background (Appendix Table 1A).

Comparing the $[H_2]$ we measured (Appendix Table 1A) to TEAP levels (Chapelle et al., 1997): Spring SpW2 had values ranging from the cusp of the NO_3^-- and Fe(III)-reducing regimes (0.2 nM) to the high side of the SO_4^{2-}-reducing range (4 nM); Spring NWSp had $[H_2] = 0.2$ nM, placing it in the NO_3^-- to Fe(III)-reducing regimes; Well NU18 had $[H_2] = 0.5$ to 0.8 nM, placing it in the Fe(III)-reducing regime; and the Hillcrest Well had $[H_2] = 0.7$ nM, placing it in Fe(III)-reducing regime as well. Based on the high $[NO_3^-]$ in SpW2

and NU18, as well as the high concentrations of the denitrification intermediate N_2O (Appendix Table 1B), a large part of the electron flow in these settings almost certainly is by denitrification, so the $[H_2]$ values we measured did not clearly reflect a major process occurring in these sample locations. The $[H_2]$ we measured in NWSp would place it in the Fe(III)-reducing TEAP regime; this TEAP classification seems inconsistent with the detection of O_2 in this water (Appendix Table 1A). The $[H_2]$ we measured in our most reducing sample location, the Hillcrest well, would place this sample in a reasonable TEAP regime based on the chemistry we measured.

4. ASCERTAINING Fe(III) SOLUBILITY CONTROL

Repeated measurements of [Fe(III)] and pH in the acidified saprolite suspension from the end of day 1 through day 6 revealed stable values corresponding to $pK_{HFO} = 40.5$, where HFO designates hydrous ferric oxides and K_{HFO} is defined according to:

$$pK_{HFO} = -\log[Fe^{3+}][OH^-]^3 \qquad (1)$$

For these computations, the small effect of complexation with OH^- and Cl^- was corrected for using complexation data supplied in Macalady et al. (1990). Our value of pK_{HFO} fits toward the midrange of values identified for synthetic HFOs that were aged between 12 and 200 h in a study by Macalady et al. (1990). This value also agrees well with a mean pK = 40.9 measured for natural HFOs from several aquifers reported by Grenthe et al. (1992).

Natural systems commonly are observed to be supersaturated with respect to thermodynamically stable minerals, the solutions preferentially equilibrating with metastable phases that have lower surface-free energies and which recrystallize over time to more stable solids in a process called Ostwald ripening (Steefel and van Cappellen, 1990; Chadwick and Chorover, 2001). In the case of HFOs, highly soluble solids are the first to precipitate (PPT) with $pK_{PPT} \sim 37$ (Langmuir and Whittemore, 1971; Macalady et al., 1990), and only then does recrystallization proceed during the subsequent 12 to 200 h to more stable forms having solubilities similar to those observed in natural systems such as our experimental value of $pK_{HFO} = 40.5$ (Macalady et al., 1990). Based on these data and this evidence, the forward reaction for oxidation of Fe(II) to precipitate Fe(III) solids is taken to be represented by freshly precipitated HFOs having the value $pK_{PPT} = 37$.

5. REDOX-COUPLE AND SATURATION-INDEX CALCULATIONS

Redox potentials were calculated for 16°C, approximately the mean temperature measured at Spring SpW2. Except as noted otherwise below, analytical data were speciated as a function of pH using the Lawrence-Livermore thermodynamic database (Bethke, 1998). These data, adjusted to activities using the Debye-Huckel Equation (Stumm and Morgan, 1996), were used to calculate redox potential in terms of pe, the negative log of electron activity that is analogous to pH. For a specific redox reaction, say:

$$NO_3^- + 2H^+ + 2e^- \rightarrow NO_2^- + H_2O \qquad (2)$$

Table 1. Redox couples

Equation	Condition	Eqn. #
$pe(O_2/H_2O) = (88.65 + \log a_{O2} - 4pH)/4$		4
$pe(O_2/H_2O_2) = (26.32 + \log a_{O2} - \log a_{H2O2} - 2pH)/2$		5
$pe(H_2O_2/H_2O) = (59.6 + \log a_{H2O2} - 2pH)/2$		6
$pe(NO_2^-/N_2O) = (48.30 + \log a_{NO2-} - 0.5\log a_{N2O} - 3pH)/2$		7
$pe(NO_3^-/NO_2^-) = (28.48 + \log a_{N3O-} - \log a_{NO2-} - 2pH)/2$		8
$pe(NO_3^-/NH_4^+) = (122.5 + \log a_{NO3-} - \log a_{NH4+} - 10pH)/8$		9
$pe(NO_2^-/NH_4^+) = (96.06 + \log a_{NO2-} - \log a_{NH4+} - 8pH)/6$		10
$pe(Fe(OH)_2^+/Fe^{2+}) = 19.20 + \log a_{Fe(OH)2+} - \log a_{Fe2+} - 2pH$	pH < 6.7	11
$pe(Fe(OH)_3^0/Fe^{2+}) = 25.76 + \log a_{Fe(OH)3} - \log a_{Fe2+} - 3pH$	pH > 6.7	12
$pe(Fe(OH)_{3PPT}/Fe^{2+}) = 18.47 - \log a_{Fe2+} - 3pH$		13
$pe(SO_4^=/H_2S) = (41.42 + \log a_{SO4=} - \log a_{H2S} - 8pH)/8$	pH < 7.0	14
$pe(SO_4^=/HS^-) = (34.21 + \log a_{SO4=} - \log a_{HS-} - 9pH)/9$	pH > 7.0	15
$pe(H_2CO_3^*/CH_4) = (22.02 + \log a_{H2CO3*} - \log a_{CH4} - 8pH)/8$	pH < 6.4	16
$pe(HCO_3^-/CH_4) = (28.45 + \log a_{HCO3-} - \log a_{CH4} - 9pH)/9$	pH > 6.4	17
$pe(H_2CO_3^*/CO) = (-5.13 + \log a_{H2CO3*} - \log a_{CO} - 2pH)/2$	pH < 6.4	18
$pe(HCO_3^-/CO) = (1.33 + \log a_{HCO3-} - \log a_{CO} - 3pH)/3$	pH > 6.4	19
$pe(H_2O/H_2) = (-3.30 - \log a_{H2} - 2pH)/2$		20
$pe(H_2CO_3^*/C_{org}) = (0.5352 + \log a_{H2CO3*} - \log a_{Corg} - 4pH)/4$	pH < 6.4	21

with log K = 28.48 (Bethke, 1998), pe is given by

$$pe = \frac{\log K}{n} + \frac{1}{n}\log\frac{\Pi a_i^v(oxidized)}{\Pi a_i^v(reduced)} = \frac{28.48}{2} + \frac{1}{2}\log\frac{a_{NO_3^-}a_{H^+}^2}{a_{NO_2^-}} \quad (3)$$

where n is the number of electrons exchanged, a_i^v is activity of species i raised to its stoichiometric coefficient v, and the activity of water is 1. The standard state for pe is the standard hydrogen electrode, $P_{H2} = 1$ atm and $a_{H+} = 1$ (Nordstrom and Munoz, 1985).

Since N exists in several oxidation states, pe was computed for conventional nitrification ($NH_4^+ \rightarrow NO_2^-$; $NH_4^+ \rightarrow NO_3^-$) and denitrification ($NO_3^- \rightarrow NO_2^- \rightarrow N_2O \rightarrow N_2$) routes. Thermodynamic data for N_2O reported in Weast (1984) and Wilhelm et al. (1977) were used to calculate this species' redox potential.

The reduction of O_2 to H_2O proceeds in several steps with intermediate product H_2O_2, i.e., $O_2 \rightarrow H_2O_2 \rightarrow H_2O$. For some time there has been no literature consensus as to whether pe for O_2 reduction is best characterized as a single value for the composite reaction to H_2O, $pe_{O2/H2O}$, or as two values, $pe_{O2/H2O2}$ and $pe_{H2O2/H2O}$ (Drever, 1988). However, recent detailed work strongly supports that H_2O_2 reduction is slow enough that the reduction of O_2 is best expressed in two steps (e.g., King and Farlow, 2000), $O_2 \rightarrow H_2O_2$ and $H_2O_2 \rightarrow H_2O$. Because H_2O_2 was not measured in this study, the mean of 111 groundwater measurements of $[H_2O_2] = 20.2$ nM (range was 3.6–44.6 nM; Holm et al., 1987) is assumed. Log-K data for the H_2O_2-half-cell reaction reported in Stumm and Morgan (1996) were used for H_2O_2 calculations.

Based on the reasoning described in Section 4, the forward reaction for oxidation of Fe(II) to form Fe(III) solids is taken to precipitate HFOs having the value $pK_{PPT} = 37$.

Given the right conditions, some organic matter can undergo direct oxidation without first undergoing fermentation. Following the method and using the thermodynamic data of Morel and Hering (1993), we coarsely modeled this degradation by treating C_{org} as $1/6$ $C_6H_{12}O_6$ (glucose) degrading fully to CO_2.

The equations used to calculate pe are summarized in Table 1.

6. THERMODYNAMIC RESULTS

Figure 1A depicts calculated pe for two years' data at the monitored spring. This figure shows that pe values remain remarkably stable through time and reveals two tightly packed clusters with a few divergent couples. The upper cluster, at pe ≈ 10, is comprised of the couples NO_3^-/NO_2^-, NO_3^-/NH_4^+, and NO_2^-/NH_4^+ clustered together with $Fe(OH)_{3PPT}/Fe^{2+}$, $Fe(OH)_2^+/Fe^{2+}$ and O_2/H_2O_2. A lower cluster also is apparent, centered at pe ≈ -2, which includes $H_2CO_3^*/CH_4$, $SO_4^=/H_2S$ and H_2O/H_2. Similar clustering is evident for the other sample locations of this study as well (Fig. 2).

With each cluster generally spanning ~ 3 pe units, couples within each cluster are close to mutual equilibrium compared to (1) the stability field for water, which is ~ 21 pe units, and 2) the free energy that microbes typically leave untapped due to constraints required to fuel their metabolism, according to Thauer et al. (1977), microbes typically leave about -2.8 kcal/mol unused. If we treat the energy gap between $pe_{NO3-/NO2-}$ and $pe_{Fe(OH)3PPT/Fe2+}$ (Fig. 1a) as though it results from the autotrophic reduction of NO_3^- with Fe^{2+} as the electron donor (Straub and Buchholz-Cleven, 1998), the reaction can be given as:

$$NO_3^- + 2Fe^{2+} + 5H_2O \rightarrow NO_2^- + 2Fe(OH)_{3PPT} + 4H^+ \quad (22)$$
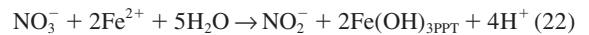
for which the free energy (ΔG_{NO2-}) is given by

$$\Delta G_{NO2-} = \Delta G_{NO2-}^o + RT \ln \frac{a_{NO2-}a_{H+}^4}{a_{NO3-}a_{Fe2+}^2} \quad (23)$$

where ΔG_{NO2-}^o is the standard state free energy, R is the universal gas constant, T is temperature in kelvin, and a_x is activity for species x. Using the thermodynamic data represented by the equations in Table 1, the standard-state free energy is $\Delta G_{NO2}^o = 11,190$ cal/mol. For Spring SpW2, the energy gap calculated for Eqn. 23 typically is -3.6 kcal/mol, ~ 1.3 times the maximum biologic end point. Hence, the energetic gaps depicted within the clusters (Fig. 1a)
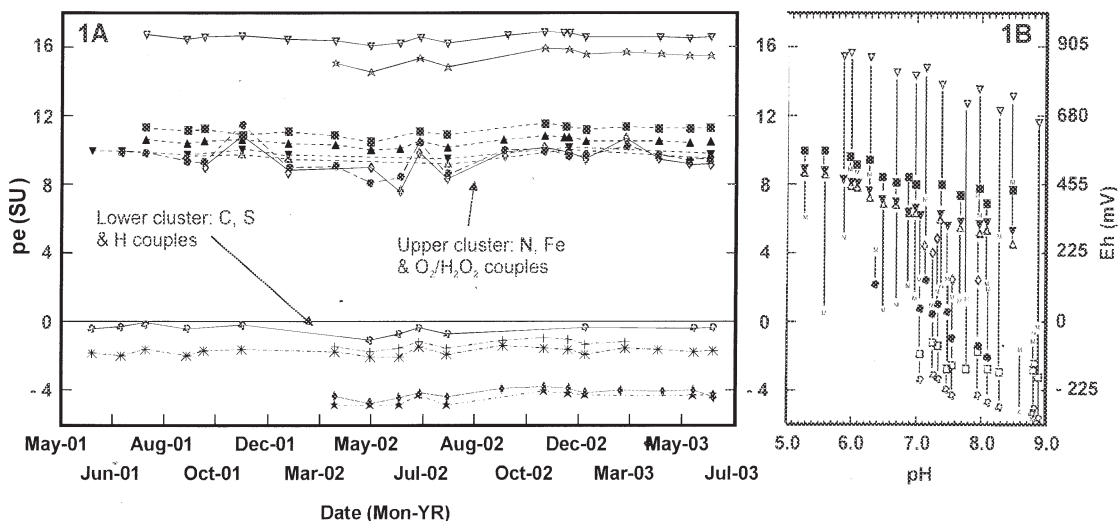
Fig. 1A. pe vs time in monitored spring. These data constitute the most extensive redox characterization of a groundwater system of which we are aware. Two stable, tight clusters persisting for two years is strong evidence of near-equilibrium between couples within clusters. Fig. 1B. pe vs pH from Lindberg and Runnells (1984). Note similarity of clusters for both studies. Symbols are consistent between 1A and 1B: $\triangledown$ O_2/H_2O; $\blacktriangle$ O_2/H_2O_2; $\blacksquare$ NO_3^-/NO_2^-; $\star$ NO_2^-/N_2O; $\blacktriangledown$ NO_3^-/NH_4^+; $\triangle$ NO_2^-/NH_4^+; $\bullet$ $Fe(OH)_3/Fe^{2+}$ ($Fe(OH)_{3PPT}$ for this study); $\diamond$ $Fe(OH)_2^+/Fe^{2+}$ (Fe^{3+} for Lindberg and Runnells (1984)); $\circ$ $SO_4^=/H_2S$ (HS^- for Lindberg and Runnells (1984)); $+$ $H_2CO_3^*/CH_4$ (HCO_3^- for Lindberg and Runnells (1984)); $\star$ $H_2CO_3^*/CO$; $*$ H_2O/H_2; $\blacklozenge$ $H_2CO_3^*/C_{org}$; $\square$ $S_{rhombic}/HS^-$; $\times$ N_2/NH_4^+; M measured.

are on the order of that typically left unused in microbial processes.

Figure 1b is a reproduction from Lindberg and Runnells (1984) used to illustrate the "near-complete lack of internal thermodynamic redox equilibrium." While it is true that redox couples commonly are discrepant among each other, comparison of data from this study (Fig. 1a) with the national database study (Lindberg and Runnells, 1984) (Fig. 1b) accentuates the patterns present in the distribution of pe values from both studies. In Figure 1a and b, the N couples tend to cluster at moderate pe values, the S couples are present at slightly negative values of pe, and the O_2/H_2O couple is present at divergent high values of pe.

All together, Figure 1a and b and Figure 2 show that patterns of pe values, identified clearly in the large database for the monitored spring, are present in the other sites of this study as well as the national study (Lindberg and Runnells, 1984). This observation reconciles that good consistency can be present for selected groupings/settings (Berner, 1963; Thorstenson, 1970; Nordstrom et al., 1979; Postma and Jakobsen, 1996; Hoehler et al., 1998) despite the huge discrepancies identified in the national study (Lindberg and Runnells, 1984). Yet, this observation also raises the questions: why do couples cluster around specific potentials; why do the compositions of these clusters seem to vary between settings; and why do some couples remain divergent?

7. DISCUSSION

Looking at the thermodynamic data depicted in Figures 1 and 2, a large gap in potential is present between the H_2, and Fe and N potentials. This gap does not support that PETEAP is the dominant redox process for these couples at these sites. In contrast, the potentials we calculated for SO_4^{2-} and methanogenesis are close to those we calculated for H_2. These patterns among couples are similar to those found by Hoehler et al. (1998) for their lab experiments with naturally reducing sediments. Hoehler et al. (1998) found that, when NO_3^-, Mn(IV), and Fe(III) were added to their reducing sediments, energetic gaps persisted between potentials calculated for H_2 and those calculated for the amendments. However, potentials calculated for [H_2] agreed closely with those calculated for sulfate reduction, methanogenesis and acetogenesis.

To the extent the LPE model holds true, deviation of redox couples from mutual equilibrium ought to be a function of reactant concentration (Morel and Hering, 1993). If this theory is correct, then Figure 3, plotting calculated electron potential
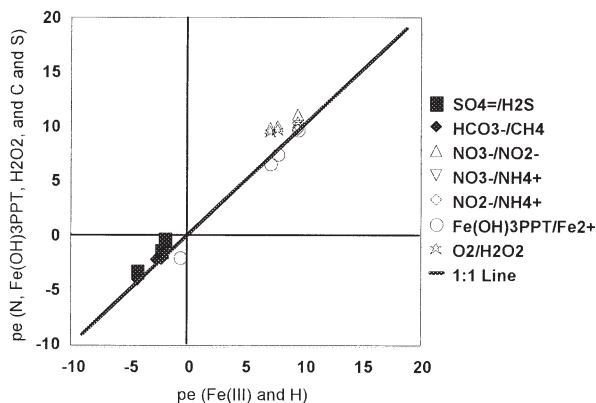

Fig. 2. Illustration that redox clustering occurs at all study sites: addressing the open symbols, N couples, O_2/H_2O_2, and $Fe(OH)_{3PPT}/Fe^{2+}$ (y axis) are plotted against $Fe(OH)_2^+/Fe^{2+}$ couples (x axis). Addressing the closed symbols HCO_3^-/CH_4 and $SO_4^=/H_2S$ couples (y axis) are plotted against H_2O/H_2 couples (x axis).
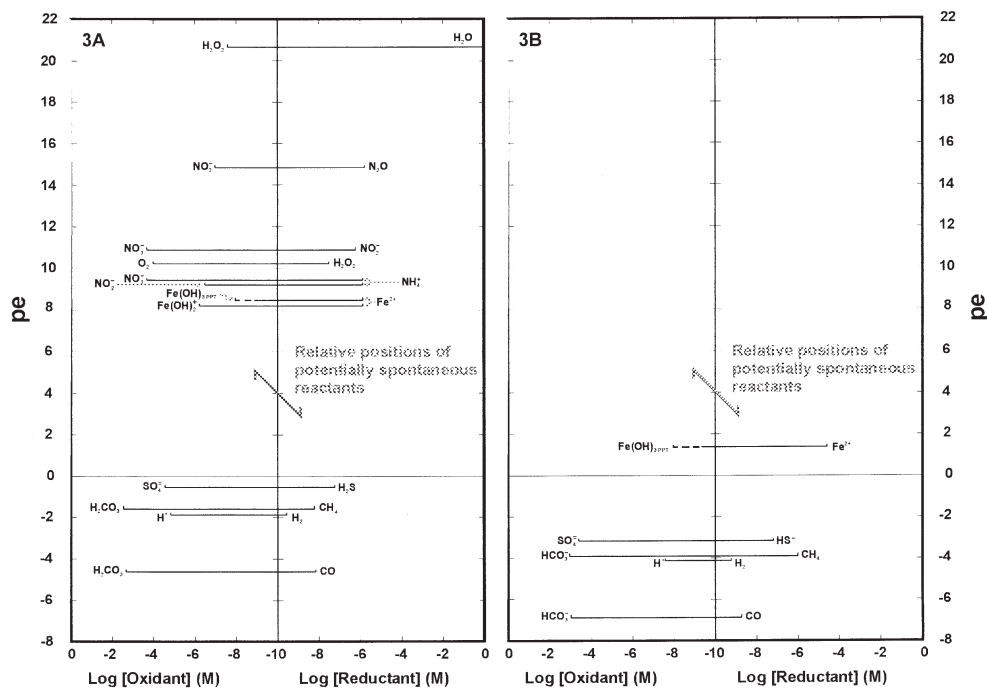
Fig. 3. A: log concentration vs pe for monitred spring. O_2 and NO_3^- react with the most concentrated reductant, Fe^{2+}, to form an oxidized cluster. Note the remarkable consistence in potentials for the fully aqueous $Fe(III)/Fe^{2+}$ and the $Fe(OH)_{3PPT}/Fe^{2+}$ that was experimentally defined as part of this study. B: log concentration vs pe for deep well having no quantifiable O_2 nor oxidized species of N. The $Fe(OH)_{3PPT}/Fe^{2+}$ couple is depicted in B to be consistent with other sample locations, but in the absence of quantifiable oxidants, there is no evidence that this freshly precipitated solid is present. Calculation of pe for a thermodynamically stable ferric oxide, say Fe_2O_3/Fe^{2+}, would place the Fe couple at about $pe_{Fe2O3/Fe2^+} = -3.1$ (thermodynamic data not shown), very close to the $pe_{SO4=/HS^-}$ couple.

vs. measured log oxidant and reductant concentrations, should be instructive for elucidating two constraints that lead to these patterns and help answer the above questions:

1. Oxidants react spontaneously only with reductants of lower potential, and reductants react spontaneously only with oxidants of higher potential. A critical extension of this simple constraint is that higher-potential oxidants and reductants generally impose no restraint on lower-potential oxidants from reacting with still lower-potential reductants.

2. In resource-limited settings, common in natural subsurface environments, both abiotic and biotic reaction rates are roughly first order in reactants (Zubay, 1993; Cachon et al., 1995; Stumm and Morgan, 1996). Consequently, oxidants commonly react dominantly with reductants that are present in highest concentration, and vice versa for reductants with oxidants, but only with those satisfying constraint 1.

Illustrating these constraints, $Fe(OH)_2^+$ is not reduced spontaneously by NO_2^- because NO_2^- is present at higher potential (Fig. 3A). Reaction of these two solutes would only pull these couples further from mutual equilibrium. However, despite the presence of NO_3^- and NO_2^-, $Fe(OH)_2^+$ can be reduced spontaneously by H_2S, CH_4, H_2, and CO (Yao and Millero, 1996; Asai et al., 1997; Fredrickson et al., 1998; Daniel et al., 1999; Zhang et al., 1999; Li et al., 2003). Hence, when other variables are held constant, the rate of $Fe(OH)_2^+$ reduction is given by:

$$\frac{\partial [Fe(OH)_2^+]}{\partial t} \approx [Fe(OH)_2^+]\{k_{H2S}^{Fe(OH)2+}[H_2S] + k_{CH4}^{Fe(OH)2+}[CH_4]$$

$$+ k_{H2}^{Fe(OH)2+}[H_2] + k_{CO}^{Fe(OH)2+}[CO]\} \quad (24)$$

where $k_X^{Fe(OH)2+}$ is the $Fe(OH)_2^+$ reduction-rate constant for reductant X. Since rate constants and reactant concentrations both can vary over orders of magnitude, the rate at which Eqn. 24 and similar reactions proceed potentially vary considerably as a function of either *rate constant* or *reactant concentration*.

In terms of rate equations, this is the point of divergence between the CETEAP and LPE models. The CETEAP model proposes that redox reaction rates vary dominantly as a function of variability in enzymatically mediated rate constants of oxidants with the fermentation intermediates such as H_2 (Lovley and Klug, 1983), generally in the order $k_{H2}^{NO3-}>k_{H2}^{Mn(IV)}>k_{H2}^{Fe(III)}>k_{H2}^{SO4=}$. Reaction of oxidants with most other reductants, whether it be abiotic or autotrophic, is not addressed directly in the CETEAP model. In contrast, the LPE model has it that rate constants for multiple reactants are sufficiently large to allow fast reactions for concentrated reactants relative to advection rates through pores (Morel and Hering, 1993; Lichtner, 1996). Consequently, redox couples composed of concentrated reactants achieve nearly thermodynamic equilibrium concomitantly, and those with dilute reactants deviate from equilibrium by an amount roughly inverse to their concentrations.

For example, our measurements indicate that $[H_2S]/[X] \geq 10$

(Fig. 3A), where X is reductant CH_4, H_2, and CO. It follows that, so long as $k_X^{Fe(OH)2+}/k_{H2S}^{Fe(OH)2+} << 10$, then Eqn. 24 is approximated by:

$$\frac{\partial [Fe(OH)_2^+]}{\partial t} \approx k_{H2S}^{Fe(OH)2+}[H_2S][Fe(OH)_2^+] \qquad (25)$$

In its most general form, this relationship implies that so long as the concentration of any one reductant exceeds that of other reductants by more than is compensated by the reduction rate constants, the oxidant is drawn toward equilibrium primarily with that reductant—in this case, $Fe(OH)_2^+$ dominantly would react with H_2S.

Offsetting this reduction of Fe(III), the oxidation rate of Fe^{2+} can be similarly characterized by its reaction with the highest concentration oxidant of higher potential, NO_3^- per Figure 3A, by:

$$\frac{d[Fe^{2+}]}{dt} \approx k_{NO3-}^{Fe2+}[NO_3^-][Fe^{2+}] \qquad (26)$$

Since $[Fe^{2+}]>[Fe(OH)_2^+]$ and $[NO_3^-]>>[H_2S]$ (Fig. 3A), Eqn. 26 will tend to proceed more quickly than will Eqn. 25 and the $Fe(OH)_2^+/Fe^{2+}$ potential can be expected to trend upward toward equilibrium with the NO_3^-/NO_2^- couple rather than downward toward the $SO_4^=/H_2S$ potential, just as observed (Fig. 3A).

Elaborating further on these arguments, although the $H_2CO_3^*/CO$ couple is closely proximate to the lower cluster, further review of Figure 3A reveals that the oxidants of the upper cluster, $[NO_3^-]$ and $[O_2]$, are much more concentrated than those of the lower cluster, $[SO_4^=]$ and $[H^+]$. Thus, it is likely that the CO oxidation rate is controlled more by $[NO_3^-]$ or $[O_2]$ than by $[SO_4^=]$ or $[H^+]$, and the $H_2CO_3^*/CO$ couple should be thought of as divergent from the upper cluster. In Figure 3A, NO_3^- and O_2 have the combined characteristics of being among the most concentrated and sufficiently oxidizing species to act as the universal end point toward which all measured reductants will be drawn. In contrast, no single measured reductant has the combined characteristics of sufficiently high concentration and low potential to act as the universal reductant for all oxidized species. For example, Fe^{2+} is concentrated, but its couple also is relatively high in potential, so it can draw N species and O_2 toward equilibrium but does not affect lower-potential oxidants directly. For these lower-potential oxidants, other less concentrated, but, critically, lower-potential reductants than Fe act as the primary reductants. Present at $\sim 10^{-5}$ M, C_{org} is among the primary reductants at potentials lower than Fe^{2+}, but characterization of its potential and molecular concentration is not straightforward; consequently, we did not plot C_{org} in Figure 3.

Figure 3B depicting data for the deep well shows that, in the absence of quantifiable O_2 and oxidized N, pe values generally are lower and the gap separating Fe from the C, S, and H couples narrows significantly. Accompanying the generally lower pe values of the Hillcrest well compared to SpW2 (Fig. 3A and B), the pH of the Hillcrest well is higher than SpW2 (Appendix Table 1A).

Given the distinct conceptual differences between the CETEAP and LPE models, these data reported herein offer the opportunity to test the merits of each theory: to the extent LPE controls redox speciation, a plot of concentration vs. deviation from equilibrium should give a pattern in which highly concentrated solutes are near equilibrium and, as solute concentration diminishes, deviation from equilibrium increases. Conversely, if CETEAP dominates redox-couple speciation, such a plot should yield a random, shotgun-blast pattern.

Figure 4 plots measured concentration of each solute against the difference in its pe value from the pe value of its most concentrated complementary reactant, i.e., the most concentrated lower-potential reductant for oxidized solutes and the most concentrated higher-potential oxidant for reduced solutes. The consistence of the pattern shown in Figure 4 with that posited for the LPE model is striking and strongly supports the LPE model.

The only reactant that deviates from the pattern posited for the LPE model is H_2. Despite being present at $[H_2] < 10^{-9}$ M, the potential for $H_2 \rightarrow H^+$ is very close to thermodynamic equilibrium with the most concentrated oxidant of higher potential, that being dissolved CO_2 being reduced to CH_4 (Fig. 3); this pattern is present for all four sample sites. The significance of this pattern is dubious, however, because: (1) CO_2-reductive methanogenesis is thought to take place only in anoxic systems (Chapelle, 1993); (2) the energetic difference between these couples equates to a free energy that is much less than that thought necessary to sustain cell metabolism (Thauer et al., 1977); and (3) the position of these H_2 data deviate from the pattern established by all other data in Figure 4. If the H_2 data are plotted against the next most concentrated oxidant (Fig. 3A), they conform more closely with the general pattern for all other data in Figure 4.

Regarding O_2 reduction, both, $pe_{O2/H2O2}$ and $pe_{H2O2/H2O}$ conform with the general pattern formed by all other couples (Fig. 4). These observations support that O_2 reduction is best characterized in two steps that account for H_2O_2 in these natural systems.

In Figure 1, we modeled C_{org} as glucose degrading to $H_2CO_3^*$; however, the true free energy of the C_{org}, or whether it actually is undergoing fermentation, is uncertain. To the extent our approximation of $pe_{H2CO3*/Corg}$ is correct (Fig. 1), its deviation from the dominant complementary reactants and the relationship depicted in Figure 4 implies that our measured atomic concentration of $[C_{org}] \sim 10^{-5}$ M equates to a molecular concentration of $\sim 10^{-7}$ to 10^{-8} M. In turn, this estimate suggests an average molecular size of about C_{100} to C_{1000}. This size is in a realistic range for dissolved C_{org} in freshwater systems (Repeta et al., 2002).

Figure 4 shows that the calculated pes for [reactants] $>10^{-6}$ M always are within four pe units of their most concentrated complementary reactant, a small difference relative to the stability field for water and to biologically mediated endpoints, which describes LPE among these reactants. Furthermore, for [reactants] $<10^{-6}$ M, these differences in pe increase roughly log-linearly with decreasing reactant concentration. In some cases, this gives rise to deviations from both clusters, in other cases the couple is part of the other cluster (Fig. 4), the potential being controlled by the more concentrated species in the couple. The observed increase in pe differences with decreasing reactant concentration is consistent with the concentration-rate-limiting hypothesis described by Eqn. 24–26. Given these patterns, this study suggests that reactions of higher-potential oxidants with lower-potential reductants com-
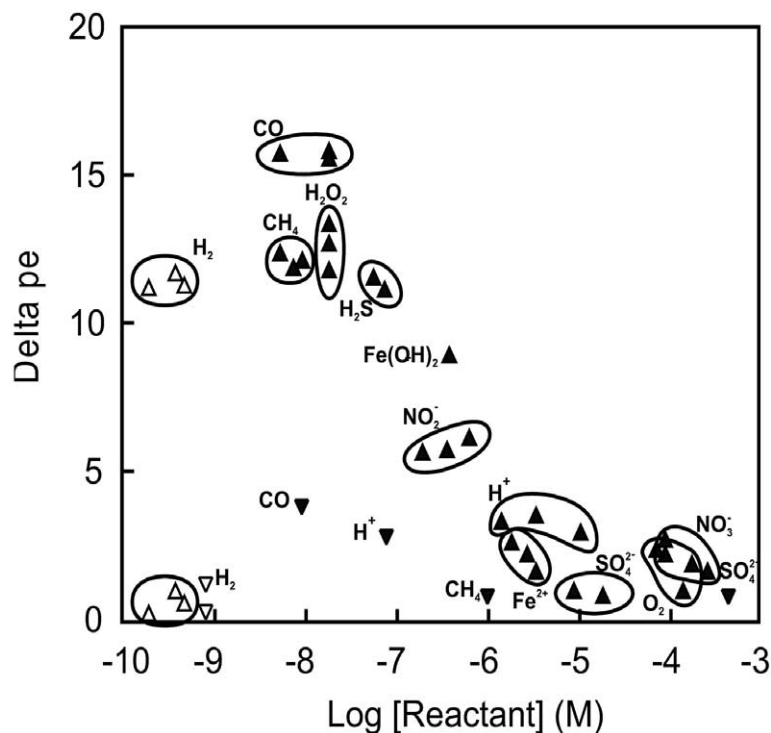
Fig. 4. pe from the dominant complementary reactant vs log measured solute concentration; see text for detailed explanation. Up-pointing triangles depict data for samples having quantifiable O_2, the 3 shallower sample locations. Down-pointing triangles depict data for the deep-source sample that had no quantifiable O_2. At concentrations $>10^{-6}$ M, pe consistently is small. At concentrations $<10^{-6}$ M, pe trends upward. For the deep sample, pe values trend upward at a gentler slope than those of the shallow sample points and all pes are less than 5, suggesting a system closer to redox consistence among all measured couples in the absence of quantifiable concentrations of O_2 and NO_3^-. Closed symbols conform to the general pattern. Open symbols are plotted twice due to questions regarding the dominant oxidant; see text for details.

monly proceed simultaneously, regardless of the presence of other reactants, with the rates of reaction being determined more by concentration than relative potentials.

With regard to modeling, these results (Fig. 4) suggest high-concentration solutes, $>10^{-6}$ M for this study, can be modeled as near equilibrium with dominant complementary reactants consistent with LPE concepts. The consistence we observed in calculated redox among H, C, and S is compatible, with PETEAP being among the dominant processes for these couples. However, our data did not support that PETEAP dominated reactions involving O_2, N and, when these high-potential oxidants were present, Fe. For low-concentration solutes, $<10^{-6}$ M in this study, the small scatter of the data along the roughly linear slope in Δpe-vs-log concentration space suggests that the variability among pseudofirst-order-rate constants commonly affects redox-reaction rates less than the variability among reactant concentrations in natural systems.

In the past, the practical utility of LPE has been limited by our knowledge of which reactions approach equilibrium. This work suggests guidance for this limitation: when high-potential oxidants (i.e., O_2, NO_3^-) and low-potential reductants (e.g., C_{org}) both are present, two clusters of potentials will be favored, and the cluster toward which a couple will tend is controlled largely by whether oxidant or reductant is present in higher concentration. As high-potential oxidants are depleted, couples are drawn primarily toward the reducing cluster. When concentrations are high, $>10^{-6}$ M in our study, reactions pro-

ceed to near equilibrium, but at lower concentrations, reactions deviate from the potential of the primary complementary reactants by an amount that is log-linearly proportional to their concentration.

Associate editor: M. L. Machesky

REFERENCES

Amirtharajah A., Young M. H., Pennell K. D., Steiner J. L., Fisher D. S., and Endale D. M. (2002) *Field Transport of Cryptosporidium Surrogate in a Grazed Catchment.* AWWA Research Foundation.

Asai S., Nakamura H., and Aikawa H. (1997) Absorption of hydrogen sulfide into aqueous ferric chloride solutions. *J. of Chem. Engineering of Japan* **30,** 500–506.

Berner R. A. (1963) Electrode studies in hydrogen sulfide in marine sediments. *Geochim. Cosmochim. Acta* **27,** 563–575.

Bethke C. M. (1998) *The Geochemist's Workbench.* University of Illinois.

Cachon R., Daniel S., and Divies C. (1995) Proton-dependent kinetics of citrate uptake in growing cells of *Lactococcus lactis* subsp. *lactis* bv. *diacetylactis. FEMS Microbiology Letters* **131,** 319–323.

Chadwick O. A. and Chorover J. (2001) The chemistry of pedogenic thresholds. *Geoderma* **100,** 321–353.

Chapelle F. H. (1993) *Ground-Water Microbiology & Geochemistry.* John Wiley & Sons, Inc.

Chapelle F. H., Vroblesky D. A., Woodward J. C., and Lovley D. R. (1997) Practical considerations for measuring hydrogen concentrations in groundwater. *Environmental Science & Technology* **31,** 2873–2877.

Clesceri L., Greenberg A., and Eaton A. (1998) Standard Methods for the Examination of Water and Wastewater. American Public Health Association.

Conrad R. and Seiler W. (1985) Influence of temperature, moisture and organic carbon on the flux of H_2 and CO between soil and atmosphere: field studies in subtropical regions. *J. of Geophysical Research* **90,** 5699–5709.

Daniel R., Warneke F., Potekhina J., and Gottschalk G. (1999) Identification of the syntrophic partners in a coculture coupling anaerobic methanol oxidation to Fe(III) reduction. *FEMS Microbiology Letters* **180,** 197–203.

Drever J. I. (1988) *The Geochemistry of Natural Waters.* Prentice Hall.

Driscoll F. G. (1989) *Groundwater and Wells.* Johnson Filtration Systems, Inc.

Fredrickson J. K., Zachara J. M., Kennedy D., Dong H., Onstott T. C., Hinman N. W., and Li S. L. (1998) Biogenic iron mineralization accompanying the dissimilatory reduction of hydrous ferric oxide by a groundwater bacterium. *Geochim. Cosmochim. Acta* **62,** 3239–3257.

Grenthe I., Stumm W., Laaksuharju M., Nilsson A.-C., and Wikberg P. (1992) Redox potentials and redox reactions in deep groundwater systems. *Chem. Geol.* **98,** 13119.

Hoehler T. M., Alperin M. J., Albert D. B., and Martens C. S. (1998) Thermodynamic control on hydrogen concentrations in anoxic sediments. *Geochim. Cosmochim. Acta* **62,** 1745–1756.

Holm T., George G., and Barcelona M. (1987) Fluorometric determination of hydrogen peroxide in groundwater. *Analytical Chemistry* **59,** 58219.

King D. W. and Farlow R. (2000) Role of carbonate speciation on the oxidation of Fe(II) by H_2O_2. *Marine Chemistry* **70,** 201–209.

Langmuir D. and Whittemore D. O. (1971) Variations in the stability of precipitated ferric oxyhydroxides. In *Nonequilibrium Systems in Natural Water Chemistry* (ed. R. F. Gould), Vol. **106,** pp. 209–234, American Chemical Society.

Li P., Miser D., Yadav R., and Hajaligol M. (2003) The removal of carbon monoxide by iron oxide nanoparticles. *Applied Catalysis B-Environmnental* **43,** 151–162.

Lichtner P. (1996) Continuum formulation of multicomponent-multiphase reactive transport. In *Reactive Transport in Porous Media* (ed. P. Lichtner et al.), Vol. 34, pp. 1–82, Mineralogical Society of America.

Lindberg R. D. and Runnells D. D. (1984) Ground water redox reactions: an analysis of equilibrium state applied to Eh measurements and geochemical modeling. *Science* **225,** 925–927.

Lovley D. R. and Goodwin S. (1988) Hydrogen concentrations as an indicator of the predominant terminal electron-accepting reactions in aquatic sediments. *Geochim. Cosmochim. Acta* **52,** 2993–3003.

Lovley D. R. and Klug M. J. (1983) Sulfate reducers can outcompete mathanogens at freshwater sulfate concentrations. *Applied and Environmental Microbiology* **45,** 187–192.

Lovley D. R. and Phillips E. J. P. (1987) Competitive mechanisms for inhibition of sulfate reduction and methane production in the zone of ferric iron reduction in sediments. *Applied and Environmental Microbiology* **53,** 2636–2641.

Lovley D. R., Coates J. D., Blunt-Harris E. L., Phillips E. J. P., and Woodward J. C. (1996) Humic substances as electron acceptors for microbial respiration. *Nature* **382,** 445–448.

Macalady D. L., Langmuir D., Grundl T., and Elzerman A. (1990) Use of model-generated Fe^{3+} ion activities to compute Eh and ferric oxyhydroxide solubilities in anaerobic systems. In *Chemical Modeling of Aqueous Systems II* (eds. D. Melchior and R. L. Bassett), pp. 350–367, American Chemical Society.

Mazur C. S. and Jones W. J. (2001) Hydrogen concentrations in sulfate-reducing estuarine sediments during PCE dehalogenation. *Environmental Science & Technology* **35,** 4783–4788.

McNab W. W. and Narasimhan T. N. (1994) Modeling reactive transport of organic compounds in groundwater using a partial redox disequilibrium approach. *Water Resources Research* **30,** 2619–2635.

Morel F. and Hering J. (1993) *Principles and Applications of Aquatic Chemistry.* John Wiley & Sons, Inc.

Mosier A. R. and Mack L. (1980) Gas chromatographic system for precise, rapid analysis of nitrous oxide. *Soil Science Society of America J.* **44,** 1121–1123.

Nordstrom D. K. and Munoz J. L. (1985) *Geochemical Thermodynamics.* Benjamin/Cummings Publishing Company.

Nordstrom D. K., Jenne E. A. and Ball J. W. (1979) Redox equilibria of iron in acid mine waters. In *Chemical Modeling in Aqueous Systems: Speciation, Sorption, Solubility and Kinetics* (ed. E. A. Jenne), Vol. **93,** pp. 51–80, American Chemical Society.

Postma D. and Jakobsen R. (1996) Redox zonation: equilibrium constraints on the Fe(III)/SO_4-reduction interface. *Geochim. Cosmochim. Acta* **60,** 3169–3175.

Railsback L. B., Bouker P. A., Feeney T. P., Goddard E. A., Hall A. S., Jackson B. P., McClain A. A., Orsega M. C., Rafter M. A., and Webster J. W. (1996) A survey of the major-element geochemistry of Georgia groundwater. *Southeastern Geol.* **36,** 99–122.

Repeta D. J., Quan T. M., Aluwihare L. I., and Accardi A.-M. (2002) Chemical characterization of high molecular weight dissolved organic matter in fresh and marine waters. *Geochim. Cosmochim. Acta* **66,** 955–962.

Rickard D. T. (1974) Kinetics and mechanism of sulfidation of goethite. *American J. of Science* **274,** 941–952.

Singer P. C. and Stumm W. (1970) Acidic mine drainage: the rate-determining step. *Science* **167,** 1121–1123.

Steefel C. I. and van Cappellen P. V. (1990) A new kinetic approach to modeling water-rock interaction: the role of nucleation, precursors and Ostwald ripening. *Geochim. Cosmochim. Acta* **54,** 2657–2677.

Stevens T. (1997) Lithoautotrophy in the subsurface. *FEMS Microbiology Rev.* **20,** 327–337.

Stookey L. L. (1970) Ferrozine—a new spectrometric reagent for iron. *Analytical Chemistry* **42,** 779–781.

Straub K. L. and Buchholz-Cleven B. E. E. (1998) Enumeration and detection of anaerobic ferrous iron-oxidizing, nitrate-reducing bacteria from diverse European sediments. *Applied and Environmental Microbiology* **64,** 4846–4856.

Stumm W. and Morgan J. J. (1996) *Chemical Equilibria and Rates in Natural Waters.* John Wiley & Sons.

Thauer R. K., Jungermann K., and Decker K. (1977) Energy conservation in chemotrophic anaerobic bacteria. *Bacteriological Rev.* **41,** 100–180.

Thorstenson D. C. (1970) Equilibrium distribution of small organic molecules in natural waters. *Geochim. Cosmochim. Acta* **34,** 74519.

Viollier E., Inglett P. W., Hunter K., Roychoudhury A. N., and Van Cappellen P. (2000) The ferrozine method revisited: Fe(II)/Fe(III) determination in natural waters. *Applied Geochemistry* **15,** 785–790.

Weast R. C. (1984) *CRC Handbook of Chemistry and Physics.* CRC Press, Inc.

Wilhelm E., Battino R., and Wilcock R. J. (1977) Low-pressure solubility of gases in liquid water. *Chem. Rev.* **77,** 219–262.

Yao W. S. and Millero F. J. (1996) Oxidation of hydrogen sulfide by hydrous Fe(III) oxides in seawater. *Marine Chemistry* **52,** 1–16.

Zhang C., Stapleton R. D., Zhou J., Palumbo A. V., and Phelps T. J. (1999) Iron reduction by psychotrophic enrichment cultures. *FEMS Microbiology Ecology* **30,** 367–371.

Zubay G. (1993) *Biochemistry.* William C. Brown Publishers.

Table 1A. Analytical data

Date	Flow rate (mL/min)	Specific conduct. (uS) y	1s	pH (SU) y	1s	Temp. (C) y	1s	[O$_2$] (mol/L) y	1s	[H$_2$] (mol/L) y	1s	Alk. Equiv. [HCO$_3$−] (mol/L) y	1s	[H$_2$CO$_3$] (mol/L) y	1s	[CO] (mol/L) y	1s	[CH$_4$] (mol/L) y	1s	[C$_{org}$] (mol/L)(2) y	1s
Spring W2																					
11/16/2000	99	79.2				12.9															
11/21/2000	355	72.3				11.3															
01/19/2001	2825	67.8		5.03		12.4						<2E-004									
02/01/2001	3850	69.5	0.1	4.97	0.12	11.9	0.1					<2E-004									
02/06/2001	3780																				
03/22/2001	22500	104.9	1.6	4.52		13.4						<2E-004									
03/28/2001	13500	88.2	0.3	4.49	0.03	13.1	0.1					<2E-004									
04/11/2001	13600	83.6				13.7															
04/17/2001	14100	79.3		4.56		14.4						<2E-004									
06/06/2001	13200	79.6	0.6	4.63	0.08	17.4	0.0			1E-009	5E-010	<2E-004				7E-009	7E-010				
07/11/2001	9232	76.6	7.1	4.54	0.11	19.8	0.2			4E-009		<2E-004				2E-008	3E-009			5E-005	1E-006
07/25/2001	90000																				
08/08/2001	13903	98.2	1.3	4.45	0.16	21.7	0.1	1E-004	5E-006	9E-010		<2E-004									
09/26/2001	8067	80.6	2.7	4.72	0.06	21.0	0.1	2E-004	3E-006	1E-009	1E-010	<2E-004				1E-008	2E-009			4E-005	1E-006
10/16/2001	6600	76.4	1.2	4.62	0.05	19.8	0.1	2E-004	2E-005	7E-010	4E-010	<2E-004				1E-008	8E-010	3E-009	1E-009	2E-005	2E-006
11/29/2001	4350	73.9	0.6	4.55	0.04	17.7	0.0	2E-004	9E-006	7E-010	6E-010	<2E-004								1E-005	1E-006
12/06/2001																				2E-005	2E-006
01/23/2002	4350	73.9	0.6	4.81	0.06	13.4	0.1	2E-004	7E-006			<2E-004				2E-009	6E-010	2E-009	1E-009	6E-005	1E-006
03/19/2002	15295	64.8	0.1	4.87	0.01	13.1	0.1	3E-004	4E-006	3E-010	1E-010	<2E-004		7E-004	6E-005	5E-009	2E-009	5E-009	9E-010	2E-005	2E-007
04/30/2002	6333	76.9	0.3	5.18	0.03	16.1	0.0	2E-004	7E-006	2E-010	2E-010	<2E-004		6E-004	5E-005	1E-009	5E-010	4E-009	1E-009	2E-005	2E-006
06/03/2002	3450	64.9	0.2	4.95	0.04	17.6	0.0	2E-004	2E-006	7E-010	1E-010	<2E-004		1E-003	2E-005	5E-009	6E-010	4E-009	2E-009	1E-005	1E-006
06/25/2002	2386	75.4	2.0	4.61	0.07	18.8	0.0	2E-004	2E-006	3E-010	1E-010	<2E-004		1E-003	2E-005	2E-009	3E-010	4E-009	2E-009	4E-005	3E-006
07/29/2002	807	76.4	0.5	4.93	0.06	20.6	0.0	2E-004	6E-006	4E-010	1E-010	<2E-004		1E-003	8E-006	6E-009	3E-010	6E-009	2E-009	6E-005	9E-007
08/29/2002	118	DRY																			
10/02/2002	1215	82.6	0.5	4.50	0.06	21.3	0.0	2E-004	1E-006	3E-010	6E-011	<2E-004		2E-003	3E-005			5E-009	7E-010	4E-005	2E-006
11/20/2002	6600	91.8	0.9	4.31	0.02	18.5	0.0	2E-004	4E-006	1E-009	5E-010	<2E-004		9E-004	2E-005	2E-009	2E-010	5E-009	1E-009	4E-005	1E-006
12/12/2002		87.6	0.0	4.43	0.00	16.0	0.0	2E-004				<2E-004								7E-005	2E-006
12/18/2002	9690	89.2	0.4	4.42	0.04	15.4	0.0	2E-004	4E-006	1E-009	5E-010	<2E-004		8E-004	3E-005	2E-009	8E-010	5E-009	7E-010	3E-005	2E-006
01/07/2003	12680	86.9	1.5	4.61	0.04	14.1	0.1	2E-004	7E-006	2E-009	4E-010	<2E-004		7E-004	6E-005	1E-009	1E-010	3E-008	4E-009	4E-005	3E-006
02/24/2003	17454	83.7	0.2	4.54	0.02	12.7	0.1			5E-010	5E-010	<2E-004		9E-004	9E-005			9E-009	4E-009	5E-005	2E-006
04/03/2003	20000	81.8	0.4	4.64	0.05	14.5	0.0	2E-004	6E-006	5E-010	2E-010	<2E-004		8E-004	3E-005					4E-005	2E-006
05/12/2003	22667	81.5	0.8	4.73	0.03	16.4	0.1	2E-004	2E-005	5E-010	4E-010	<2E-004		9E-004	2E-005	1E-009	5E-010			2E-005	1E-006
06/05/2003	24000	80.2	0.4	4.73	0.01	17.5	0.0	2E-004	5E-006	3E-010	2E-010	<2E-004		9E-004	1E-004	7E-010	8E-011			2E-004	5E-006
NW Spring																					
02/26/2002	−2000	32.3	0.3	5.34	0.11	14.3	0.1	2E-004	2E-006			4E-004		6E-004	4E-005	1E-008	2E-009			2E-005	2E-006
03/07/2002	−2000	31.8	0.3	5.41	0.02	14.1	0.1	2E-004	6E-006	2E-010	9E-011	4E-004		5E-004	6E-005	2E-008	1E-009	1E-008	2E-009		
Well NU18																					
05/08/2002	−140	57.8	0.1	5.80	0.01	20.1	0.1	8E-005	1E-006	5E-010	5E-010	5E-004		8E-004	6E-005	2E-008	3E-008	8E-009	1E-009	2E-004	2E-006
06/05/2002	−140	45.6	0.7	5.34	0.02	22.0	0.4	2E-004	8E-006	8E-010	2E-010	<2E-004		8E-004	2E-005	2E-008	8E-009	5E-009	9E-010	1E-004	8E-007
Hillcrest Well																					
07/23/2002	1.1E + 006	232.5	0.3	7.09	0.11	18.7	0.1	<9E-006		7E-010	4E-010	1E-003	3E-004	3E-004		2E-009	2E-010	1E-006	3E-008	5E-005	2E-006

(1) 6/25/2002 values for NO$_3^-$, Cl$^-$, SO$_4^=$, and NH$_3$ are for samples collected 6/26/2002.

(2) Standard deviations for this analyte represent only analytical error, whereas; other standard deviations reflect variability between multiple samples as well.

Redox buffering

J. W. Washington, D. M. Endale, L. P. Samarkina, and K. E. Chappell

Table 1B. More analytical data

Date	[NO$_3^-$] (mol/L) y	1s	[NO$_2^-$] (mol/L) y	1s	[N$_2$O] (mol/L) y	1s	[NH$_4^+$] (mol/L) y	1s	[SO$_4^=$] (mol/L) y	1s	[H$_2$S] (mol/L) y	1s	[Fe(II)] (mol/L) y	1s	[Fe(III)] (mol/L) y	1s	[Cl^{-1}] (mol/L) y	1s	[H$_2$PO$_4^{-1}$] (mol/L)
Spring W2																			
11/16/2000	3E-004	2E-005							3E-005	2E-006							1E-004	3E-006	<2E-006
11/21/2000	3E-004	5E-006							2E-005	7E-007							1E-004	2E-006	<2E-006
01/19/2001																			
02/01/2001	3E-004	4E-006							1E-005	5E-007							2E-004	2E-006	<2E-006
02/06/2001																			
03/22/2001	1E-004	7E-006							6E-006	1E-007							1E-004	5E-006	<2E-006
03/28/2001																			
04/11/2001																			
04/17/2001																			
06/06/2001	3E-004	7E-005					<6E-007		3E-006	4E-007	3E-008	3E-008	4E-007				2E-004	7E-006	<2E-006
07/11/2001	2E-004	0E+000					6E-007	2E-007	8E-006	8E-007	6E-008	0E+000	2E-006				2E-004	3E-007	<2E-006
07/25/2001													2E-007						
08/08/2001	2E-004	2E-005	2E-007	6E-008			<6E-007		1E-005	1E-007	3E-008	1E-008	5E-006	4E-006			2E-004	1E-005	<5E-006
09/26/2001	3E-004	6E-006	2E-007	4E-008			5E-007	4E-007	9E-006	5E-007	3E-008	0E+000	3E-006	1E-006			2E-004	5E-006	<5E-006
10/16/2001	3E-004	9E-005	2E-007	4E-008			<3E-006		1E-005	5E-006	<3E-008		6E-006	3E-006	9E-007	3E-007	2E-004	7E-005	<5E-006
11/29/2001	2E-004	3E-005	6E-007	0E+000			<6E-007	0E+000	1E-005	2E-006	3E-008	3E-008	5E-008	2E-008	<4E-007		1E-004	2E-005	<5E-006
12/06/2001	3E-004								2E-005								2E-004		<5E-006
01/23/2002	4E-004	1E-004	2E-007	0E+000			<6E-007	0E+000	2E-005	6E-006	<3E-008		4E-006	3E-006	8E-007	7E-007	3E-004	9E-005	<5E-006
03/19/2002	2E-004	2E-005	2E-007	4E-008	4E-007	2E-008	<3E-006		6E-006	4E-007	<3E-008		2E-006	1E-006	<5E-007		1E-004	2E-005	<5E-006
04/30/2002	1E-004	2E-005	2E-007	4E-008	8E-007	7E-008	<4E-007		7E-006	7E-007	5E-008	2E-008	2E-006	2E-006	3E-006	5E-006	9E-005	1E-005	<1E-007
06/03/2002	3E-004	3E-005	<2E-007		1E-006	1E-007	<4E-007		9E-006	9E-007	3E-008	3E-008	5E-006	3E-006	<4E-007		2E-004	2E-005	<5E-006
06/25/2002	2E-004	5E-005	2E-007	4E-008	2E-006	1E-007	<6E-007		9E-006	3E-006	4E-008	4E-008	4E-007	3E-007	4E-007	3E-007	1E-004	3E-005	<5E-006
07/29/2002	3E-004	7E-006	2E-007	2E-008	1E-006	2E-008	6E-007	2E-008	2E-005	3E-006	6E-008	3E-008	4E-006	3E-006	4E-007	2E-007	2E-004	4E-006	<5E-006
08/29/2002																			
10/02/2002	4E-004	1E-006	<2E-007		8E-007	4E-008	<6E-007		2E-005	1E-006	<3E-008		3E-006	3E-006	1E-006	2E-007	2E-004	1E-006	<5E-006
11/20/2002	6E-004	2E-006	2E-007	5E-008	5E-007	3E-008	<6E-007		8E-006	1E-006			8E-006	6E-006	4E-006	4E-006	3E-004	3E-006	<5E-006
12/12/2002			2E-007	0E+000															<1E-007
12/18/2002	5E-004	4E-006	4E-007	0E+000	4E-007	2E-008	7E-007	2E-007	8E-006	7E-008	<3E-008		1E-005	2E-006	4E-006	1E-006	3E-004	4E-006	<5E-006
01/07/2003	5E-004	2E-006	3E-007	2E-008	4E-007	4E-008	<6E-007		8E-006	8E-007	1E-007	3E-008	3E-006	2E-006	1E-006	1E-006	3E-004	2E-006	<5E-006
02/24/2003	5E-004	1E-006	2E-007	4E-008	2E-007	1E-008	<6E-007		8E-006	5E-007	<3E-008		1E-006	2E-006	6E-006	1E-005	3E-004	2E-006	<1E-007
04/03/2003	4E-004	1E-006	3E-007	0E+000	4E-007	1E-008	<6E-007		8E-006	2E-007	<3E-008		2E-006	2E-006	9E-007	4E-007	3E-004	6E-007	<1E-007
05/12/2003	4E-004	1E-006	2E-007	0E+000	5E-007	3E-008	<6E-007		9E-006	2E-006	5E-008	0E+000	3E-006	2E-006	9E-007	1E-006	3E-004	4E-006	<5E-006
06/05/2003	4E-004	6E-006	2E-007	0E+000	4E-007	2E-009	8E-007	6E-008	9E-006	4E-007	3E-008	0E+000	2E-006	7E-007	4E-007	3E-007	3E-004	6E-006	<5E-006
NW Spring																			
02/26/2002	6E-005	2E-005	3E-007	7E-008	2E-007	3E-009	<3E-006		7E-006	2E-006	8E-008	2E-008	2E-006	9E-008	<4E-007		6E-005	2E-005	<5E-006
03/07/2002	1E-004	6E-006	4E-007	4E-008	2E-007	8E-009	<3E-006		1E-005	1E-006	8E-008	2E-008	3E-006	1E-006	<5E-007		1E-004	5E-006	<5E-006
Well NU18																			
05/08/2002	1E-004	6E-006	7E-007	7E-008	5E-006	3E-007	<4E-007		7E-006	6E-007	<3E-008		2E-006	2E-006	<4E-007		2E-005	1E-006	<5E-006
06/05/2002	3E-004	1E-004	3E-007	2E-008	1E-006	1E-007	<4E-007		4E-006	2E-006	<3E-008		9E-006	5E-006	2E-006	1E-006	5E-005	2E-005	<5E-006
Hillcrest Well											[HS$^-$]								[HPO$_4^=$]
07/23/2002					1E-008	5E-009	4E-006	5E-008	4E-004	4E-005	5E-008	2E-009	2E-005	2E-006	<4E-007		9E-005	1E-005	1E-005

(1) 6/25/2002 values for NO$_3^-$, Cl$^-$, SO$_4^=$, and NH$_3$ are for samples collected 6/26/2002.

(2) Standard deviations for this analyte represent only analytical error, whereas other standard deviations reflect variability between multiple samples as well.